Molecular design of triarylamine-based organic dyes for efficient dye-sensitized solar cells

Gang Li,[ab] Ke-Jian Jiang,*[a] Peng Bao,[a] Ying-Feng Li,[a] Shao-Lu Li[a] and Lian-Ming Yang*[a]

Received (in Gainesville, FL, USA) 8th September 2008, Accepted 17th December 2008
First published as an Advance Article on the web 3rd February 2009
DOI: 10.1039/b815649b

Three donor–(π-spacer)–acceptor dyes, coded as **DS-3**, **DS-5** and **DS-6**, were designed and synthesized for dye-sensitized solar cells (DSSCs). These dyes possess the same donor (triarylamine) and acceptor/anchoring group (2-cyanoacrylic acid), but the varied π-spacers consisting of a combination of thiophene and/or 3,4-ethylenedioxythiophene (EDOT) units. They were evaluated by photophysical and electrochemical measurements as well as in nanocrystalline TiO_2-based DSSCs fabricated using them as light-harvesting sensitizers. The results showed that incorporation of the EDOT moiety in the dye molecules strongly affected the molar extinction coefficient and photocurrent response. Among the three dyes, the **DS-5**-based DSSCs afforded the best photovoltaic performance: a maximum monochromatic incident photon-to-current conversion efficiency (IPCE) of 80%, a short-circuit photocurrent density (J_{sc}) of 14.6 mA cm^{-2}, an open-circuit photovoltage (V_{oc}) of 0.59 V and a fill factor (*FF*) of 0.70, corresponding to an overall conversion efficiency of 6.03% under 100 mW cm^{-2} irradiation, which reached 77% with respect to that of an N3-based device fabricated and measured under similar conditions. Further, a method of molecular orbital calculations was employed for the insight into the geometrical, electronic and optical properties of these dyes.

Introduction

Since the seminal publication of Grätzel and co-workers in 1991,[1] dye-sensitized solar cells (DSSCs) have attracted considerable interest because of their higher conversion efficiency of sunlight-to-electricity and potential low costs of production and materials as compared to conventional silicon-based solar cells. Typically, DSSCs are composed of a photoactive TiO_2 anode coated with photosensitizers (sensitizing dyes), redox electrolytes and a passive cathode (n-type DSSCs).[2] In such devices, the sensitizing dye must be adsorbed chemically onto the surface of nanocrystalline mesoporous TiO_2. Upon light illumination, the adsorbed dye becomes an excited state and then the excited dye injects electrons into the conduction band of TiO_2. The electrons are brought back to the oxidized dye through an external circuit, a passive cathode and a redox electrolyte system (typically I^-/I_3^-), regenerating the oxidized sensitizing dye.

Among all the elements of DSSCs, the photosensitizer is fundamental to the cell's performance and stability. Sensitizing dyes for DSSCs are divided generally into two types, inorganic metal complexes and metal-free organic dyes. Although inorganic dyes, such as Ru complexes (N3, N719 and black dyes),[3–5] can provide efficient solar energy-to-electricity conversion efficiencies of up to 10%, the Ru sources and the resulting environmental issues would greatly limit their applications outdoors. In recent years, metal-free organic dyes as an alternative to the noble metal complexes have been attracting increasing attention because of the following advantages: easy preparation; low costs and little environment issues; high molar extinction coefficient; and a wider variety of structures, *etc*. Generally, a good organic sensitizing dye must meet some basic requirements: (1) the HOMO energy level should be sufficiently lower than the corresponding redox couple (electrolytes, *e.g.*, I^-/I_3^-) so that the dye can be quickly regenerated from its oxidized state, and the LUMO energy level should be sufficiently more negative than the conduction band edge level of TiO_2 to ensure electron injection efficiently; (2) the absorption of the dye should overlap the largest possible range of the solar spectrum, especially the region from the visible to near-infrared light because the photon flux in this region is largest in the solar irradiation spectrum; and (3) the molecular structure of dye should be a D–π–A mode to facilitate charge transfer and subsequent charge separation, and to slow down the charge recombination between the injected electron and the oxidized dye. To date, remarkable advances have been made in organic dyes as photosensitizers for DSSCs. Various organic dyes, such as perylene,[6] cyanine,[7] porphyrin,[8] phthalocyanine,[9] merocyanine,[10] coumarin,[11] hemicyanine,[12] indoline[13] and triphenylamine[14] dyes, have been employed. Particularly, a high η value of 9% was achieved in full sunlight by Ito *et al*. using indoline dye as photosensitizer in DSSCs.[15] These results have shown a promising potential for organic dye-based DSSCs in practical applications.

[a] *Beijing National Laboratory for Molecular Sciences (BNLMS), Laboratory of New Materials, State Key Laboratory for Structural Chemistry of Unstable and Stable Species, Institute of Chemistry, Chinese Academy of Sciences, Beijing, 100190, P. R. China. E-mail: yanglm@iccas.ac.cn. E-mail: kjjiang@iccas.ac.cn; Fax: +86-10-62559373; Tel: +86-10-62565609*
[b] *Graduate School of Chinese Academy of Sciences, Beijing, 100049, P. R. China*

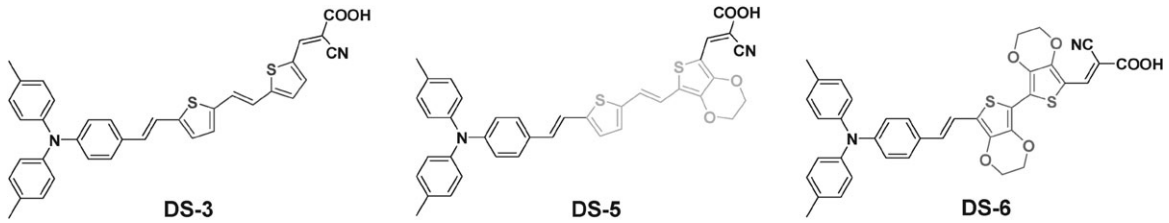

Fig. 1 Molecular structures of as-synthesized organic dyes.

Organic dyes for DSSCs consist commonly of donor, linker and acceptor (*i.e.*, D–π–A structure), and hence their various properties could be finely tuned by alternating independently or matching different parts in a D–π–A dye. Certainly, the π-spacers as bridging groups play an important role in modifying properties and performances. We were interested in introduction of 3,4-ethylenedioxythiophene (EDOT) into π-linker groups in dye molecules because EDOT is a conducting molecule and has presented some specific properties as a building block in functionalized π-conjugated systems or polymers.[16] However, EDOT has rarely been employed as the structural part of photosensitizers in DSSCs, and only an extremely low efficiency was achieved in one publication on EDOT-containing organic dye-based DSSCs.[17] Herein we wish to report our investigation into three D–π–A chromophores coded as **DS-3**, **DS-5** and **DS-6** (Fig. 1) which contain the triarylamine group as donor (D), 2-cyanoacrylic acid as acceptor (A) bridged by thiophene and/or EDOT units.

Results and discussion

Synthesis of materials

The photosensitive dyes in this study are depicted in Fig. 1. Synthetic routes to the as-synthesized organic dyes are illustrated in Scheme 1. (*E*)-1,2-Bis(5-formyl-2-thienyl)ethane reacted with *p*-(di-*p*-tolylamino)benzyltriphenylphosphonium bromide leading to compound **1** through a mono-Wittig reaction.[18] The thiophene moiety was coupled to the donor to afford compound **2** by the Wittig–Horner reaction of *p*-(di-*p*-tolylamino)benzyltriphenylphosphonium bromide and thiophene-2-carbaldehyde. The intermediate **2** was then converted to the corresponding aldehyde **3** in a moderate yield by the Vilsmeier reaction in the presence of DMF and $POCl_3$ in refluxing anhydrous dichloromethane. A second Wittig–Hornor reaction of **3** with 3,4-ethylenedioxy-2-thienyl-methyl triphenylphosphonium bromide produced **4** which was subjected to a Vilsmeier reaction to give **5**. The intermediate **7** was also prepared by a process similar to the synthesis of compound **3**. Finally, target dyes were yielded by the Knoevenagel reaction of the corresponding aldehydes with cyanoacetic acid in refluxing acetonitrile in the presence of piperidine. These target dyes were fully characterized by NMR spectroscopy, mass spectrometry and elemental analysis, and found to be consistent with the proposed structures. The obtained dyes are purple or violet in the solid state, and easily dissolved in common organic solvents, such as dichloromethane, chloroform, THF, DMF, *etc*.

Photophysical properties

The absorption spectra of the dyes in DMF solutions are displayed in Fig. 2(a), and the corresponding data are presented in Table 1. All the three dyes exhibited a π–π* transition band in the range of 300–350 nm. Moreover, they also give a strong absorption maximum (460–490 nm) in the visible region, which may be assigned to an intramolecular charge transfer (ICT) absorption because an efficient charge-separated excited state could be produced between the triarylamine and the cyanoacrylic acid moieties.[19] As seen in Table 1, the ICT absorption (λ_{max}) appeared at 473 nm for **DS-3**, 486 nm for **DS-5**, and 478 nm for **DS-6**, respectively; molar extinction coefficients at visible maxima (ε) were 34 000 M^{-1} cm^{-1} for **DS-3**, 61 000 M^{-1} cm^{-1} for **DS-5**, and 41 000 M^{-1} cm^{-1} for **DS-6**, respectively, all of which are twice as high as that of $Ru(dcbpy)_2(NCS)_2$ (N3 dye: *ca.* 1.6 × 10^4 M^{-1} cm^{-1}).[20] The ε values of **DS-5** and **DS-6** are superior to dye **DS-3** due likely to a more extensive conjugation of molecules containing the EDOT moiety. Also as seen from Fig. 2(a), the maximum absorption of **DS-5** is slightly red-shifted in comparison with that of **DS-6**, which should be attributed to a little more expansion of the **DS-5** π-system by introduction of one additional methine unit into its π-bridge. Further, the half-height absorption width of **DS-5** is remarkably larger than those of both **DS-6** and **DS-3**, and thus it is predictable that dye **DS-5** has an enhanced ability to harvest solar light.

Fig. 2(b) shows the normalized absorption and emission spectra of **DS-5** in air-equilibrated DMF solution (0.5 mM), and the data were also collected in Table 1. The excitation wavelength for emissions was 480 nm. The maximum absorption and emission in DMF are at 486 and 633 nm, respectively. On the other hand, no emission signal was observed for all three dyes on the TiO_2 colloidal electrodes, suggesting that there existed an efficient electron injection from the excited dye molecules into the conduction band of TiO_2.

The absorption spectra of the dyes absorbed onto TiO_2 nanocrystalline electrodes are shown in Fig. 3. The absorption spectra of the dyes were distinctly broadened. Such spectral broadening is favourable for harvesting visible light. Compared to the absorption spectra in solutions, the film absorptions of **DS-3** and **DS-6** show a large red-shift (**DS-3**: 34 nm; and **DS-6**: 30 nm) due to J-aggregation, while dye **DS-5** was slightly blue-shifted (from 486 to 480 nm) which could be ascribed to slight H-aggregation on the TiO_2 surface. Such aggregation phenomena have been observed in several organic dyes.[21,22] Thus, chenodeoxychlolic acid is

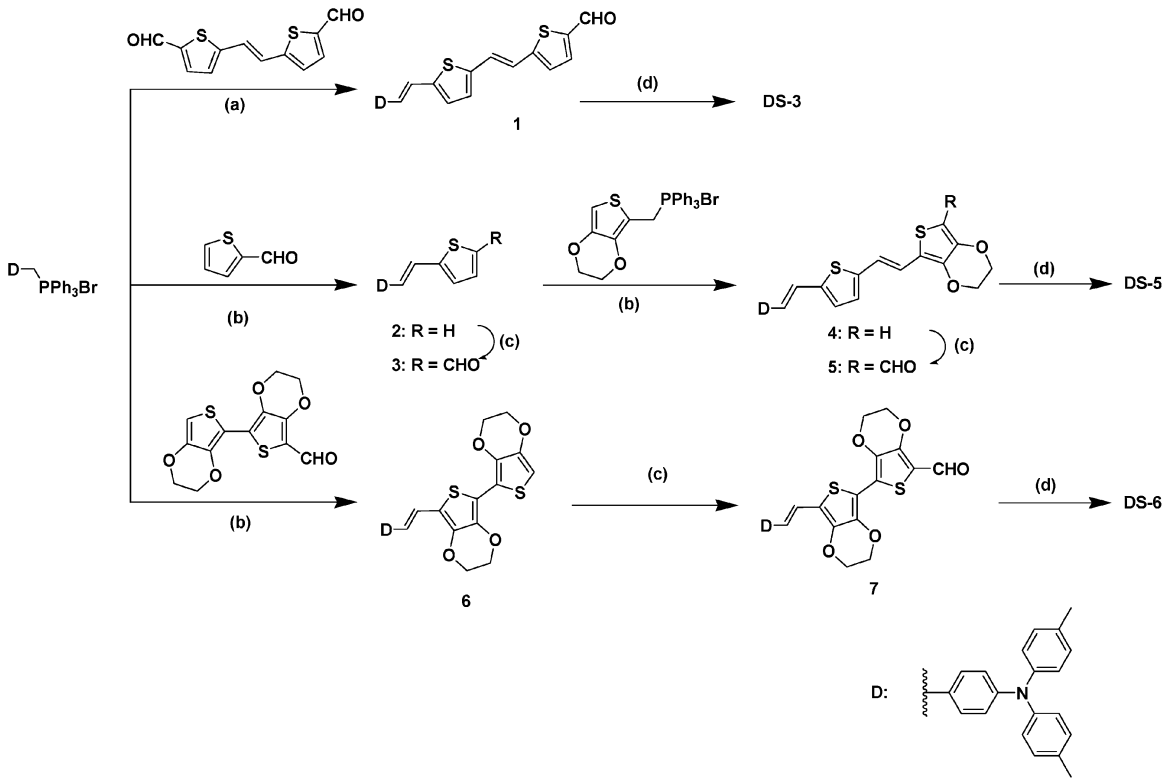

Scheme 1 Synthesis of the chromophores. *Reagents and conditions*: (a) DMF/18-crown-6, K_2CO_3, rt; (b) THF/*t*-BuOK, rt; (c) DMF/$POCl_3$, CH_2Cl_2, reflux; (d) $CNCH_2COOH$, piperidine, MeCN, reflux.

usually used as a co-adsorbent to suppress dye aggregation in DSSC assembly since dye aggregation tends to impair electron injection from the excited dye to the TiO_2.

Electrochemical properties

The electrochemical behavior of the dyes was investigated by cyclic voltammetry (CV), and the data are listed in Table 1. The oxidation potentials of the as-synthesized dyes are determined from the oxidation peak potential and reduction peak potential for the oxidation process. As seen in Fig. 4, the dyes can be reversibly oxidized at a moderately high oxidation potential under low concentration conditions. The oxidation potential *vs.* NHE (E_{ox}) corresponds to the highest occupied molecular orbital (HOMO). As listed in Table 1, the first oxidation potentials of the dyes (0.96–1.04 V *vs.* NHE) are more positive than the I^-/I_3^- redox couple ($\sim$0.4 V *vs.* NHE). The sufficiently low HOMO energy level of the dye can ensure more effective dye regeneration and restrain the recapture of the injected electrons by the dye cation radical or the I^-/I_3^- redox couple. Moreover, the oxidation potential of dye **DS-5** (1.03 V) is slightly negative than that of **DS-3** (1.04 V) likely because the former has a strong electron-donating EDOT moiety. Interestingly, dye **DS-6** (0.96 V) bearing two EDOT units attains only a relatively low oxidation potential compared to **DS-5**.

The excited state oxidation potential (E_{ox}*) of the sensitizer, corresponding to the lowest unoccupied molecular orbital (LUMO), is determined from the first oxidation potential (E_{ox}) of the ground state and the zero–zero transition energy (E_{0-0}) according to eqn (1):

$$E^*_{ox} = E_{ox} - E_{0-0} \quad (1)$$

where E_{0-0} was estimated from the intersection of the absorption and emission spectra. As listed in Table 1, the excited state potentials of the dyes (**DS-3**: −1.23 V *vs.* NHE; **DS-5**: −1.21 V *vs.* NHE; **DS-6**: −1.36 V *vs.* NHE) are much more negative than the conduction band energy level of TiO_2 (*ca.* −0.5 V *vs.* NHE), clarifying that the electron injection should be possible thermodynamically. Furthermore, the positive shift of the excited state oxidation potentials for **DS-3** and **DS-5**, compared to dye **DS-6**, can be explained by the presence of two EDOT units in DS-6 which enrich the electron density and make the molecule more easily oxidized.

Photovoltaic devices

DSSCs were fabricated using the dyes **DS-3**, **DS-5** and **DS-6**, as photosensitizers with an effective working area of 0.2 cm^2, nanocrystalline anatase TiO_2 on FTO, the electrolyte composed of 0.6 M 1-propyl-3-methylimidazolium iodide, 0.1 M LiI, 0.05 M I_2 and 0.75 M 4-*tert*-butylpyridine in a co-solvent of acetonitrile–valeronitrile (1 : 1, v/v). The action spectra of the incident photon-to-current conversion efficiency (IPCE) as a function of wavelength, which is defined as the number of electrons generated by light in the external circuit divided by the number of incident photons, is calculated using eqn (2), and the data are plotted in Fig. 5.

$$\mathrm{IPCE}(\lambda) = \frac{1240\ (\mathrm{eV\ nm})}{\lambda\ (\mathrm{nm})} \times \frac{J_{sc}\ (\mathrm{mA\ cm^{-2}})}{\varphi\ (\mathrm{mW\ cm^{-2}})} \quad (2)$$

In eqn (2), J_{sc} is the short-circuit photocurrent generated by monochromatic light, λ the wavelength of incident monochromatic light, and φ the incident light intensity.

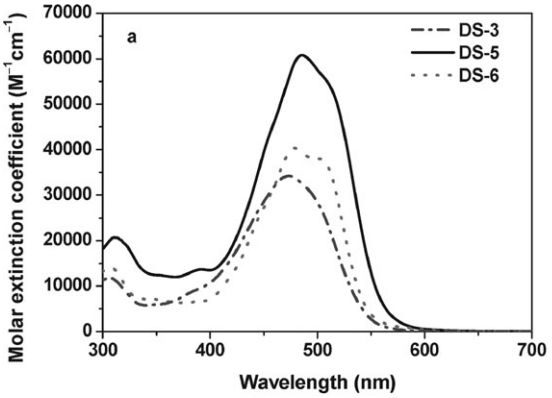

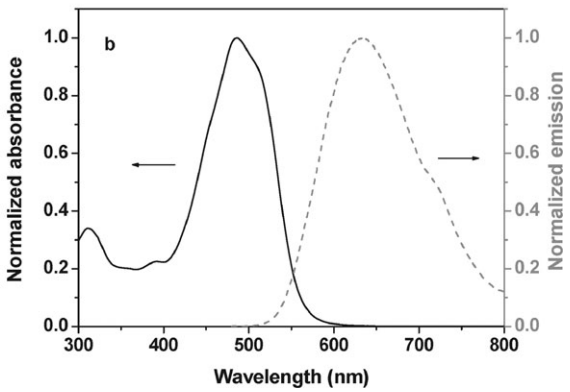

Fig. 2 (a) UV-Vis absorption spectra of organic dyes in DMF. (b) Normalized absorption (solid line) and emission (dashed line) spectra for **DS-5** in DMF.

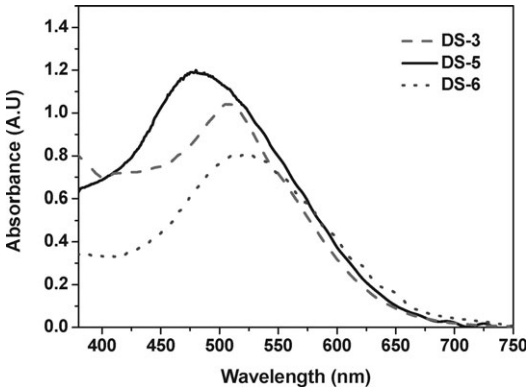

Fig. 3 Absorption spectra of the three dyes absorbed onto TiO_2 film electrodes.

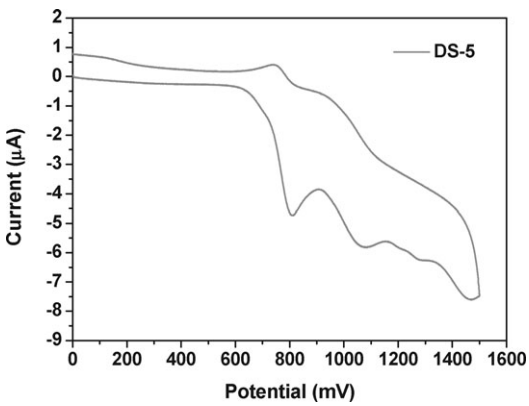

Fig. 4 Cyclic voltammetry of the dye **DS-5**. Scanning rate is 100 mV s^{-1}; working electrode and counter electrode: Pt wires; reference electrode: Hg/Hg_2Cl_2.

For **DS-5**, a high IPCE (above 70%) was obtained in the range from 400 to 560 nm with a maximum value of 80% at 480 nm; the onset of IPCE was extended to 800 nm. Considering reflection and absorption losses in the transparent conducting oxide substrate, the net photon-to-current conversion efficiency exceeds 95%, indicating a highly efficient performance of the **DS-5**-based solar cell. In the cases of **DS-3** and **DS-6**, relatively low IPCE values were observed, with maximum values of 67% at 483 nm (for **DS-3**) and 50% at 548 nm (for **DS-6**). The higher IPCE values for **DS-5** should stem from its broader absorption and enhanced molar extinction coefficient in the visible region. Relative to the dye **DS-5**, relatively low IPCE values of **DS-6** could be caused by a serious self-quenching of the electronically excited state because of *cis–trans* isomerization and the disordered alignment of chromophores in J-like aggregation.[21b]

Fig. 6 presents photocurrent density–voltage (*J–V*) curves of the cells measured under simulated solar irradiation (1 sun, 100 mW cm^{-2}, 1.5 air mass global). The open-circuit photovoltage (V_{oc}), short-circuit photocurrent density (J_{sc}), fill factor (*FF*), and solar-to-electrical energy conversion efficiencies (η) are listed in Table 1. The conversion efficiency (η) of the DSSCs is calculated from the short-circuit photocurrent density (J_{sc}), the open-circuit photovoltage

Table 1 Optical properties, redox potentials and DSSC performance of the dyes

Dye	λ_{ab}/nm[a] (ε/M^{-1} cm^{-1})[b]	λ_{ex}[c]/nm	E_{ox}[d]/V *vs.* NHE	E_{0-0}[e]/eV	E_{ox}*[f]/V *vs.* NHE	J_{sc}/mA cm^{-2}	V_{oc}/V	*FF*	η[g] (%)
DS-3	473 (34 000)	641	1.04	2.27	−1.23	11.1	0.630	0.73	5.12
DS-5	486 (61000)	633	1.03	2.24	−1.21	14.6	0.590	0.70	6.03
DS-6	478 (41000)	586	0.96	2.32	−1.36	9.46	0.585	0.65	3.59
N3						16.87	0.680	0.68	7.82

[a] Absorption spectra were measured in DMF solution at room temperature. [b] The molar absorbance coefficient of the absorption spectra at λ_{max}. [c] The maximum emission of dyes in DMF. [d] The oxidation potential of the dyes were measured in DMF with 0.1 M $(n\text{-}C_4H_9)_4NPF_6$ as electrolyte. Scan rate: 100 mV s^{-1}. Working electrode and counter electrode: Pt wires; reference electrode: Hg/Hg_2Cl_2. [e] $E_{0\text{-}0}$ was estimated from the intersection between the absorption and emission spectra. [f] The reduction potential of the dyes was calculated from $E_{ox} - E_{0\text{-}0}$. [g] Performances of the DSSCs were measured with 0.2 cm^2 working area.

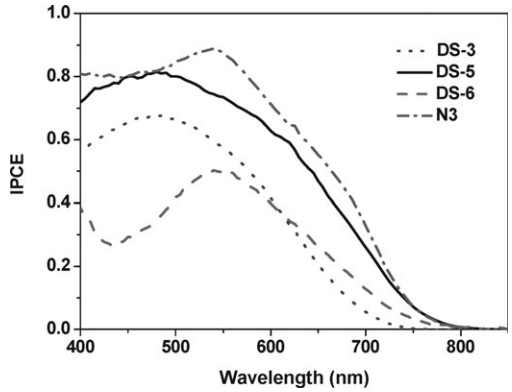

Fig. 5 Action spectra of monochromatic incident photo-to-current conversion efficiency (IPCE) of N3 and the three dye-sensitized solar cells. The electrolyte used was 0.6 M 1-propyl-3-methylimidazolium iodide, 0.1 M LiI, 0.05 M I_2 and 0.75 M 4-*tert*-butylpyridine in a co-solvent of acetonitrile–valeronitrile (1 : 1, v/v).

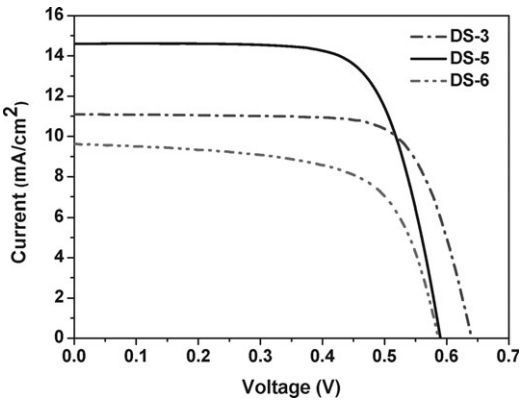

Fig. 6 Photocurrent–voltage characteristics of the three dye-sensitized solar cells under illumination of simulated solar light (AM 1.5, 100 mW cm^{-2}). The electrode used was the same as that for Fig. 5.

(V_{oc}), the fill factor (*FF*), and the intensity of the incident light (P_{in}),[23] by eqn (3):

$$\eta = \frac{J_{sc}\ (\text{mA cm}^{-2}) \times V_{oc}\ (\text{V}) \times FF}{P_{in}\ (\text{mW cm}^{-2})} \qquad (3)$$

Under solar-simulated light irradiation, the **DS-5**-sensitized solar cell shows a short-circuit photocurrent density (J_{sc}) of 14.6 mA cm^{-2}, open-circuit photovoltage (V_{oc}) of 0.59 V and fill factor (*FF*) of 0.70, corresponding to an overall energy conversion efficiency (η) of 6.03%; the **DS-3**-sensitized cell gave J_{sc} of 11.1 mA cm^{-2}, V_{oc} of 0.63 V and *FF* of 0.73, corresponding to an overall conversion efficiency η of 5.12%. Compared to the dye **DS-3**, the **DS-5**-based cell exhibits larger energy conversion efficiency due mainly to its larger short-circuit photocurrent density (J_{sc}). The reason may be that **DS-5** has both a broader absorption and a larger molar extinction coefficient in the visible region and hence could more efficiently capture the solar radiation energy. On the other hand, the **DS-6**-sensitized cell exhibited much lower photovoltaic performance compared to the **DS-3** and **DS-5** based cells, which could be attributed to its lower spectral

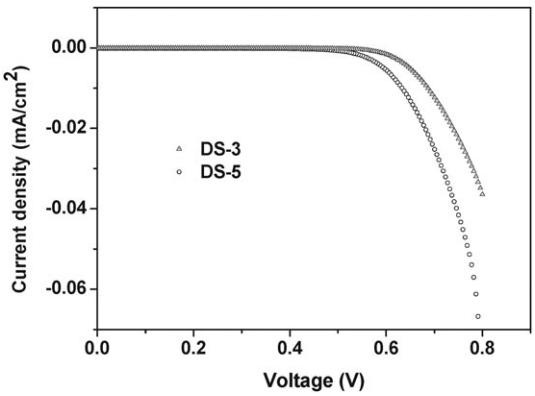

Fig. 7 Current–voltage curves obtained with the DSSCs based on **DS-3** and **DS-5** dyes under dark conditions.

response due to the strong aggregation of **DS-6** on TiO_2 films. Here, the **DS-6**-sensitized cell gave J_{sc} of 9.46 mA cm^{-2}, V_{oc} of 0.585 V and *FF* of 0.65, corresponding to only 3.59% of overall conversion efficiencies (η). For comparison, the device with standard N3 dye has J_{sc} = 16.87 mA cm^{-2}, V_{oc} = 680 mV, *FF* = 0.68 and η = 7.82% under the similar conditions. The results suggest a promising prospect of the as-synthesized organic dyes applied in DSSCs, particularly **DS-5**.

It is necessary to make a further comparison between **DS-3** and **DS-5** since they have a similar structure but display distinctly different photocurrent values. The principal factor should be that **DS-5** has better light harvesting ability (broader absorption and larger molar extinction coefficient). The dark current–voltage curves obtained from the **DS-3** and **DS-5** based DSSCs are shown in Fig. 7. **DS-5** showed a larger dark current and thus a higher degree of charge recombination mainly with the electrolyte species.[14a] So the introduction of the EDOT moiety may change the arrangement and orientation manner of dye molecules and further influence the access of electrons in TiO_2 to oxidized electrolyte. The charge recombination at the interface would directly result in low V_{oc} values.[24] Consistent with the above-mentioned dark current analyses, the open-circuit voltage (V_{oc}) value is in the order of **DS-5** < **DS-3**. On the other hand, **DS-5** can furnish a relatively higher short-circuit photocurrent density in contrast to **DS-3**. Finally the **DS-5** based photocell produced a higher conversion efficiency than that of the **DS-3**. So a suitable π-spacer should be adopted to the photosensitizer structure for the balance between V_{oc} and J_{sc} in pursuit of a superior conversion efficiency. A further study on dynamics of electron transport and recombination of DSSCs based on the two dyes are underway.

Molecular orbital calculations

To gain insight into the geometrical, electronic and optical properties of dyes, we mimicked the optimized geometries of the three dyes by the hybrid density functional theory (B3LYP) with 6-31G(D) basis set as implemented in the Gaussian 03 program.[28] The electron distributions of the HOMO and LUMO of the dyes are shown in Fig. 8. At the ground state for the dyes, electrons are homogeneously distributed in both the electron donor and π-bridge, and upon

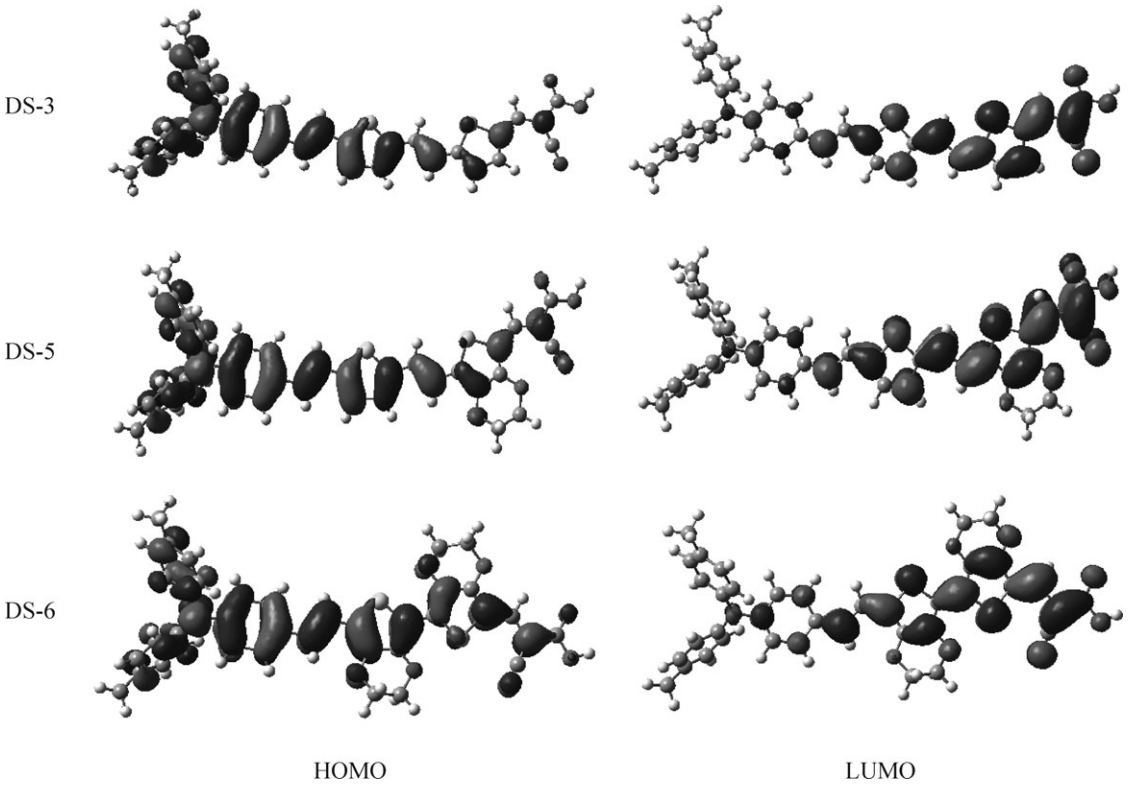

Fig. 8 Frontier orbitals of the three dyes optimized at the B3LYP/6-31G(D) level.

the light illumination, electrons move from the HOMO to the LUMO by an intramolecular charge transfer, and are finally located in anchoring groups through the π-bridge. Fig. 8 reveals that the cyanoacrylic acid group is essentially coplanar with respect to the thiophene and/or EDOT fragments in their energy minimised structures. Assuming that the dye molecule has a similar molecular orbital geometry when anchored to TiO_2, the position of the LUMO close to the anchoring group would enhance the orbital overlap with the titanium 3d orbital and thus favor electron injection from dye to TiO_2.

Conclusions

We have investigated three metal-free organic dyes (**DS-3**, **DS-5** and **DS-6**) that feature triarylamine as electron-donating moiety and cyanoacrylic acid as electron-accepting moiety bridged by thiophene and/or EDOT moieties. Introduction of the EDOT moiety could strongly affect the photocurrent response of the dyes by controlling photophysical and photovoltaic properties. Under the photovoltaic performance measurement, a maximum photo-to-electron conversion efficiency of 6.03% was achieved with the DSSC based on dye **DS-5** under AM 1.5 irradiation (100 mW cm^{-2}), which reached 77% with respect to that of an N3-based device fabricated and measured under similar conditions. Our results demonstrated the necessity and importance of designing or modifying π-spacers in D–π–A dyes for DSSCs. Further structural modification of **DS-5** for broadening the spectral absorption and increasing the molar extinction coefficient is anticipated to give some new organic dyes with even better performances.

Experimental

General

All reactions and manipulations were carried out under nitrogen atmosphere unless otherwise stated. THF was distilled from sodium/benzophenone. DMF, dichloromethane and $POCl_3$ were distilled from CaH_2. ^1H NMR spectra were obtained on a Bruker Avance 400 (400 MHz) or Bruker DMX 300 (300 MHz) spectrometer with tetramethylsilane as internal standard. ^{13}C NMR spectra were recorded on a Bruker Avance 400 (100 MHz). MALDI-TOF mass spectrometric measurements were performed on the Bruker Biflex III MALDI-TOF. Elemental analyses were performed on a FLASH EA1112 elemental analyzer. EI were recorded on the APEXII FT-ICR spectrometer. UV–Vis and fluorescence spectra of the dyes in DMF solutions were recorded in a quartz cell with 1 cm path length on an HP-8453 spectrometer and F-4500 fluorescence spectrophotometer, respectively. Potassium *tert*-butoxide, thiophene-2-carbaldehyde, tetrabutylammonium perchlorate, chenodeoxycholic acid (DCA), Triton X-100, 4-*tert*-butylpyridine (TBP), $TiCl_4$, LiI and I_2 from Aldrich, N3 from Solaronix Company, and cyanoacetic acid from TCI were used as received without further purification. 3,4-Ethylenedioxy-2-formylthiophene and 5-formyl-2,2′-bi(3,4-ethyleneoxythiophene) were synthesized according to the literature procedures.[25] All other solvents and chemicals used in this work were analytical grade and used without further purification. Chromatographic separations were carried out on silica gel (200–300 mesh). Transient conducting oxide (TCO, F–doped SnO_2, 10 Ω $\square^{-1}$, Nippon Sheet Glass)

was washed with a basic solution, ethanol, and acetone successively under supersonication for 15 min before use.

Synthesis

5-{2-[5-[*p*-Di(*p*-tolyl)aminostyryl]thiophene-2-yl]vinyl}thiophene-2-carbaldehyde (1). The synthetic procedure and characterizations were presented in an earlier publication.[18]

5-{2-[5-[*p*-Di(*p*-tolyl)aminostyryl]thiophene-2-yl]vinyl}thiophene-2-cyanoacrylic acid (DS-3). The synthetic procedure and characterizations were presented in an earlier publication.[18]

5-{2-[*p*-Di(*p*-tolyl)aminophenyl]vinyl}thiophene (2). A mixture of 4-(di-*p*-tolylamino)benzyl triphenylphosphonium bromide (3.77 g, 6 mmol) and thiophene-2-carbaldehyde (0.467 ml, 5 mmol) were dispersed in anhydrous THF (30 mL) and stirred at ambient temperature under nitrogen atmosphere for 30 min. *t*-BuOK (0.785 g, 7 mmol) was dissolved in anhydrous THF and added dropwise to the solution, the mixture was stirred overnight at ambient temperature. Then a molar excess of water was added and the mixture was extracted with CH_2Cl_2 (50 mL × 3). The combined extract was dried over anhydrous Na_2SO_4 and filtered. Solvent removal by rotary evaporation, followed by column chromatography over silica gel with a mixture of CH_2Cl_2 and petroleum (1 : 8, v/v) as eluent, yielded a yellow solid (1.42 g). This crude product was used directly in the next step without further purification. MS-EI: m/z 381 (M^+).

5-[*p*-Di(*p*-tolyl)aminostyryl]thiophene-2-carbaldehyde (3). $POCl_3$ (0.867 mL, 9.55 mmol) was added dropwise with stirring to a solution of anhydrous CH_2Cl_2 (20 mL) and anhydrous DMF (8 mL) at 0–5 °C under nitrogen atmosphere. After stirring for 30 min, a solution of compound **2** (1.42 g, 3.47 mmol) in CH_2Cl_2 (10 mL) was added slowly. The solution was allowed to warm to room temperature and then refluxed for 12 h. After cooling to room temperature, the solution was added to 50 mL of iced water and stirred for 10 min, followed by neutralization with aqueous NaOH (10%). The mixture was extracted with CH_2Cl_2, and the organic phase was washed with water, dried over Na_2SO_4, and filtered. Solvent removal by rotary evaporation, followed by column chromatography over silica gel with a mixture of ethyl acetate and petroleum ether (1 : 10, v/v) as eluent, yielded **3** as a red solid (1.0 g, 65%). ^{1}H NMR (400 MHz, $CDCl_3$): δ 2.32 (s, 6H), 6.96 (d, 2H, J = 8.67 Hz), 7.01 (d, 4H, J = 8.38 Hz), 7.05–7.08 (m, 7H), 7.31 (d, 2H, J = 8.70 Hz), 7.63 (d, 1H, J = 3.90 Hz), 9.82 (s, 1H). MS-EI: m/z 409 (M^+).

5-{2-[5-[*p*-Di(*p*-tolyl)aminostyryl]thiophene-2-yl]vinyl}-3,4-ethylenedioxythiophene (4). A mixture of 3,4-ethylenedioxy-2-thienylmethyl triphenylphosphonium bromide (1.5 g, 3 mmol) and **2** (0.82 g, 2 mmol) were dispersed in anhydrous THF (30 mL), and stirred at ambient temperature under nitrogen atmosphere for 30 min. *t*-BuOK (0.6 g, 5.3 mmol) was dissolved in anhydrous THF and added dropwise to the solution. The mixture was stirred overnight at ambient temperature, and then 20 mL water was added. The mixture was extracted with CH_2Cl_2 (10 mL × 3), and the combined extract was dried over anhydrous Na_2SO_4 and filtered. Solvent removal by rotary evaporation, followed by column chromatography over silica gel with a mixture of ethyl acetate and petroleum (1:6) as eluent, yielded a yellow solid (0.39 g). The crude product was used directly in the next step without further purification. MS-EI: m/z 547 (M^+).

5-2-[5-[*p*-Di(*p*-tolyl)aminostyryl]thiophene-2-yl]vinyl-3,4-ethylenedioxythiophene-2-carbaldehyde (5). $POCl_3$ (1 mL, 11 mmol) was added dropwise with stirring to a solution of anhydrous CH_2Cl_2 (20 mL) and anhydrous DMF (5 mL) at 0–5 °C. After stirring for 30 min, a solution of compound **4** (0.39 g, 7.12 mmol) in CH_2Cl_2 (10 mL) was added slowly, and then the solution turned brown–red. The solution was allowed to warm to room temperature, and then refluxed for 12 h. After cooling to room temperature, the solution was poured onto 50 mL of iced water, and stirred for 10 min, followed by neutralization with aqueous NaOH (10%, w/w). The mixture was extracted with CH_2Cl_2, and the organic phase was washed with water and dried over Na_2SO_4 and filtered. Solvent removal by rotary evaporation and column chromatography over silica gel with a mixture of dichloromethane and petroleum ether (2 : 1, v/v) as eluent yielded **5** as a brown–red solid (0.3 g, 73.3%). ^{1}H NMR (300 MHz, $CDCl_3$): δ 2.32 (s, 6H), 4.35–4.39 (m, 4H), 6.84 (d, 1H, J = 16 Hz), 6.85–6.99 (m, 4H), 6.97 (d, 2H, J = 9 Hz), 7.00 (d, 4H, J = 8.4 Hz), 7.08 (d, 4H, J = 8.4 Hz), 7.20 (d, 1H, J = 16 Hz), 7.27 (d, 2H, J = 9 Hz), 9.87 (s, 1H). MS-EI: m/z 575 (M^+).

5-2-[5-[*p*-Di(*p*-tolyl)aminostyryl]thiophene-2-yl]vinyl-3,4-ethylenedioxythiophene-2-cyanoacrylic acid (DS-5). The compound **5** (0.22 g, 0.38 mmol), cyanoacetic acid (0.1 g, 1.17 mmol), piperidine (0.2 mL) and acetonitrile (30 mL) was charged sequentially in a three-necked flask and heated to reflux under N_2 atmosphere for 8 h. After cooling to room temperature, solvent was removed by rotary evaporation, the solid was absorbed on silica gel and purified by column chromatography using CH_2Cl_2–acetic acid (150 : 1, v/v) as eluent, yielding the product **DS-5** as a purple solid (0.23 g, 93.6%); mp 268 °C. ^{1}H NMR (400 MHz, d_6-DMSO): δ 2.3 (s, 6H), 4.43–4.49 (m, 4H), 6.84 (d, 2H, J = 8.6 Hz), 6.90 (d, 1H, J = 10.3 Hz), 6.93–6.95 (m, 5H), 7.11–7.14 (m, 5H), 7.25 (d, 1H. J = 16 Hz), 7.30 (d, 1H, J = 3.8 Hz), 7.38 (d, 1H, J = 16 Hz), 7.42 (d, 2H, J = 8.7 Hz), 8.16 (s, 1H). ^{13}C NMR (400 MHz, d_6-DMSO): δ 20.88, 65.27, 66.40, 109.65, 116.17, 117.51, 119.90, 121.57, 125.21, 125.68, 127.93, 128.04, 129.41, 129.82, 130.58, 131.02, 133.24, 139.44, 140.13, 140.19, 144.66, 144.77, 147.98, 149.38, 164.56. MS (MALDI-TOF): m/z 642.0 (M^+). Anal. Calc. for $C_{38}H_{30}N_2O_4S_2$: C, 71.00; H, 4.70; N, 4.36. Found: C, 71.05; H, 5.02; N, 4.36%.

2-5-[*p*-Di(*p*-tolyl)aminostyryl]-3,4-ethylenedioxythiophene-2-yl-3,4-ethylenedioxythiophene (6). A mixture of [4-di(*p*-tolyl)-aminobenzyl] triphenylphosphonium bromide (2.55 g, 4.06 mmol) and 5-formyl-2,2′-bi(3,4-ethyleneoxythiophene) (0.95 g, 3.06 mmol) were dispersed in anhydrous THF (50 mL) and stirred at ambient temperature under nitrogen atmosphere for 10 min. *t*-BuOK (0.56 g, 5 mmol) was dissolved in anhydrous THF and added dropwise to the solution. The mixture was stirred overnight at ambient temperature. After a molar excess of water was added, the mixture was extracted with CH_2Cl_2

(50 mL × 3). The combined extracts were dried over anhydrous Na_2SO_4 and filtered. Solvent removal by rotary evaporation, followed by column chromatography over silica gel with a mixture of CH_2Cl_2 and petroleum ether (1 : 1, v/v) as eluent, yielded a yellow solid (1.6 g). The crude product was used directly in the next step without further purification. MS-EI: m/z 579 (M^+).

2-5-[*p*-Di(*p*-tolyl)aminostyryl]-3,4-ethylenedioxythiophene-2-yl-3,4-ethylenedioxythiophene-5-carbaldehyde (7). $POCl_3$ (0.4 mL, 4.4 mmol) was added dropwise with stirring to a solution of anhydrous CH_2Cl_2 (10 mL) and anhydrous DMF (0.32 mL) at 0–5 °C under nitrogen atmosphere. After stirring for 30 min, a solution of **6** (1.5 g, 2.58 mmol) in CH_2Cl_2 (10 mL) was added slowly. Then the solution was allowed to warm to room temperature, and refluxed for 12 h. After cooling to room temperature, the solution was poured onto 50 mL of ice–water and stirred for 10 min, followed by neutralization with aqueous NaOH (10%, w/w). The mixture was extracted with CH_2Cl_2, and the organic phase was washed with water and dried over Na_2SO_4 and filtered. Solvent removal by rotary evaporation and column chromatography over silica gel with CH_2Cl_2 as eluent yielded **7** as a red solid (0.95 g, 60%). ^{1}H NMR (300 MHz, $CDCl_3$): δ 2.31 (s, 6H), 4.32–4.42 (m, 8H), 6.85 (d, 1H, J = 16 Hz), 6.95 (d, 2H, J = 8.7 Hz), 7.00 (d, 4H, J = 8.3 Hz), 7.03 (d, 1H, J = 16 Hz), 7.06 (d, 4H, J = 8.3 Hz), 7.27 (d, 2H, J = 8.7 Hz), 9.88 (s, 1H). MS-EI: m/z 607 (M^+).

2-2-[5-[*p*-Di(*p*-tolyl)aminostyryl]-3,4-ethylenedioxy-thiophene-2-yl]-3,4-ethylenedioxythiophene-5-yl]cyanoacrylic acid (DS-6). The compound **7** (0.13 g, 0.21 mmol), cyanoacetic acid (0.1 g, 1.17 mmol), piperidine (0.2 mL) and ethanol (40 mL) was charged sequentially in a three-necked flask and heated to reflux under N_2 atmosphere for 8 h. After cooling to room temperature, solvent was removed by rotary evaporation, the residue was absorbed on silica gel and purified by column chromatography using CH_2Cl_2–acetic acid (50:1, v/v) as eluent, yielding the product **DS-6** as a dark-purple solid (0.08 g, 55%); mp 249 °C. ^{1}H NMR (400 MHz, d_6-DMSO): δ 2.3 (s, 6H), 4.39–4.49 (m, 8H), 6.81 (d, 2H, J = 8.5 Hz), 6.89 (d, 1H, J = 16 Hz), 6.94 (d, 4H, J = 8.2 Hz), 7.06 (d, 1H, J = 16 Hz), 7.13 (d, 4H, J = 8.2 Hz), 7.42 (d, 2H, J = 8.5 Hz), 8.16 (s, 1H). ^{13}C NMR (400 MHz, d_6-DMSO): δ 20.38, 64.58, 65.07, 65.38, 65.73, 105.76, 108.85, 114.94, 115.65, 117.44, 119.72, 120.87, 121.02, 124.76, 127.37, 127.94, 129.49, 130.10, 132.78, 136.19, 138.53, 139.65, 140.70, 144.28, 147.38, 148.26, 164.42. MS (MALDI-TOF): 674.1 (M^+). Anal. Calc. for $C_{38}H_{30}N_2O_6S_2$: C, 67.64; H, 4.48; N, 4.15; Found: C, 67.15; H, 4.55; N, 4.08%.

Electrochemical measurements

Electrochemical redox potentials were measured *via* cyclic voltammetry using a three-electrode cell under room temperature in DMF solutions. The working and counter electrodes were Pt wires, and the reference electrode was Hg/Hg_2Cl_2. The electrolyte was 0.1 M $(n\text{-}C_4H_9)_4NPF_6$ in DMF. The $E_{1/2}$ values were determined as $(E_{pa} + E_{pc})/2$, where E_{pa} and E_{pc} are the anodic and cathodic peak potentials, respectively. Ferrocene was added to each sample solution at the end of the experiments, and the ferrocene/ferrocenium (Fc/Fc^+) redox couple was used as an internal potential reference.

Fabrication of the dye-sensitized nanocrystalline TiO_2 electrodes

For fabrication of the devices, two layers of TiO_2, the main layer and scattering layer, were prepared by screen-printing TiO_2 pastes on FTO glass substrate (10 Ω $\square^{-1}$, Nippon Sheet Glass). The main layer (thickness: 14 μm; TiO_2 particle size: 18 nm) and scattering layer (thickness: 8 μm; TiO_2 particle size: 400 nm) were prepared from these two different TiO_2 colloids (PST-18NR and PST-400C from Catalysts & Chemicals Ind. Co., Ltd, CCIC in Japan). After screen-printing, the TiO_2 film was heated at 500 °C for 30 min, and treated with 0.04 M $TiCl_4$ aqueous solution as reported by Ito.[26] The three dyes and N3 solutions were prepared in DMF at a concentration of 0.5 mM; 1 mM chenodeoxycholic acid in *tert*-butyl alcohol–acetonitrile (1 : 1, v/v) was added as reported in order to effectively prevent unfavorable dye aggregation on the TiO_2 surface.[27] The TiO_2 films were left in solution at room temperature for 24 h. A Pt-sputtered FTO glass was used as a counter electrode. The electrolyte was composed of 0.6 M 1-propyl-3-methylimidazolium iodide, 0.1 M LiI, 0.05 M I_2 and 0.75 M 4-*tert*-butylpyridine in a co-solvent of acetonitrile–valeronitrile (1 : 1, v/v). The photovoltaic performance of the devices was recorded under 100 mW cm^{-2} simulated air mass (AM) 1.5 solar light illumination.

Photovoltaic measurements

The action spectra of monochromatic incident photon-to-current conversion efficiency (IPCE) for solar cells was performed by using a commercial setup for IPCE measurement (PV-25 DYE, JASCO) under 5 mW cm^{-2} monochromic light illumination. The irradiation source for the photocurrent–voltage (J–V) measurement is an AM 1.5 solar simulator (YSS-50A, Yamashita Denso Co. Ltd.). A 500-W Xe lamp serves as the light source in combination with a band-pass filter (400–800 nm) to remove the ultraviolet and infrared light and to give a light power of 100 mW cm^{-2}. The current–voltage curves were obtained by a linear sweep voltammetry method using an electrochemical workstation using a PC-controlled voltage–current source meter (R6246, Advantest) under a solar simulator illumination (Yamashita Denso, Yss-80) of Air Mass 1.5 (100 mW cm^{-2}) conditions at 25 °C. The active electrode area was 0.2 cm^2.

Molecular orbital calculations

All calculations were performed on the Gaussian 03 program package by using Density Functional Theory (DFT).[28] B3LYP and the 6-31 G (D) basis set were used. Before optimizing ground-state geometries by B3LYP/6-31G(D), the molecular structures were initially optimized in a HF/ST0-3G calculation method. All the geometries and electronic properties were calculated by assuming that the target molecules would be isolated in gas phase.

Acknowledgements

The authors thank the National Natural Science Foundation of China (Projects No. 20672116 and No. 20774103) for financial support of this work.

References

1 (*a*) B. O'Regan and M. Grätzel, *Nature*, 1991, **353**, 737; (*b*) M. Grätzel, *Nature*, 2001, **414**, 338.
2 W. Xu, B. Peng, J. Chen, M. Liang and F. Cai, *J. Phys. Chem. C*, 2008, **112**, 874.
3 (*a*) M. K. Nazeeruddin, A. Kay, I. Rodicio, R. H. Baker, E. Muller, P. Liska, N. Vlachopoulos and M. Grätzel, *J. Am. Chem. Soc.*, 1993, **115**, 6382; (*b*) M. K. Nazeeruddin, P. Péchy, T. Renouard, S. M. Zakeeruddin, R. H. Baker, P. Comte, P. Liska, L. Cevey, E. Costa, V. Shklover, L. Spiccia, G. B. Deacon, C. A. Bignozzi and M. Grätzel, *J. Am. Chem. Soc.*, 2001, **123**, 1613; (*c*) K.-J. Jiang, N. Masaki, J. B. Xia, S. Nodab and S. Yanagida, *Chem. Commun.*, 2006, 2460.
4 M. K. Nazeeruddin, F. De Angelis, S. Fantacci, A. Selloni, G. Viscardi, P. Liska, S. Ito, B. Takeru and M. Grätzel, *J. Am. Chem. Soc.*, 2005, **127**, 16835.
5 C. Klein, M. K. Nazeeruddin, D. D. Censo, P. Liska and M. Grätzel, *Inorg. Chem.*, 2004, **43**, 4216.
6 (*a*) S. Ferrere, A. Zaban and B. A. Gregg, *J. Phys. Chem. B*, 1997, **101**, 4490; (*b*) S. Ferrere and B. A. Gregg, *New J. Chem.*, 2002, **26**, 1155; (*c*) H. Tian, P.-H. Liu, W. Zhu, E. Gao, D.-J. Wu and S. Cai, *J. Mater. Chem.*, 2000, **12**, 2708.
7 (*a*) K. Hara, T. Sato, R. Katoh, A. Furube, Y. Ohga, A. Shinpo, S. Suga, K. Sayama, H. Sugihara and H. Arakawa, *J. Phys. Chem. B*, 2003, **107**, 597; (*b*) S. Tatay, S. A. Haque, B. O'Regan, J. R. Durrant, W. J. H. Verhees, J. M. Kroon, A. Vidal-Ferran, P. Gaviña and E. Palomares, *J. Mater. Chem.*, 2007, **29**, 3037; (*c*) S. Sreejith, P. Carol, P. Chithra and A. Ajayaghosh, *J. Mater. Chem.*, 2008, **3**, 264.
8 (*a*) M. Tanaka, S. Hayashi, S. Eu, T. Umeyama, Y. Matano and H. Imahori, *Chem. Commun.*, 2007, 2069; (*b*) W. M. Campbell, K. W. Jolley, P. Wagner, K. Wagner, P. J. Walsh, K. C. Gordon, L. Schmidt-Mende, M. K. Nazeeruddin, Q. Wang, M. Grätzel and D. L. Officer, *J. Phys. Chem. C*, 2007, **111**, 11760.
9 (*a*) J. He, G. Benkö, F. Korodi, T. Polívka, R. Lomoth, B. Åkermark, L.-C. Sun, A. Hagfeldt and V. Sundström, *J. Am. Chem. Soc.*, 2002, **124**, 4922; (*b*) P. Y. Reddy, L. Giribabu, C. Lyness, H. J. Snaith, C. Vijaykumar, M. Chandrasekharam, M. Lakshmikantam, J.-H. Yum, K. Kalyanasundaram, M. Grätzel and M. K. Nazeeruddin, *Angew. Chem., Int. Ed.*, 2007, **46**, 373.
10 (*a*) A. C. Khazraji, S. Hotchandani, S. Das and P. V. Kamat, *J. Phys. Chem. B*, 1999, **103**, 4693; (*b*) K. Sayama, K. Hara, N. Mori, M. Satsuki, S. Suga, S. Sukagoshi, Y. Abe, H. Sugihara and H. Arakawa, *Chem. Commun.*, 2000, 1173.
11 (*a*) K. Hara, Y. Tachibana, Y. Ohga, A. Shinpo, S. Suga, K. Sayama, H. Sugihara and H. Arakawa, *Sol. Energy Mater. Sol. Cells*, 2003, **77**, 89; (*b*) K. Hara, Y. Dan-oh, C. Kasada, Y. Ohga, A. Shinpo, S. Suga, K. Sayama and H. Arakawa, *Langmuir*, 2004, **20**, 4205; (*c*) K. Hara, Z.-S. Wang, T. Sato, A. Furube, R. Katoh, H. Sugihara, Y. Dan-oh, C. Kasada, A. Shinpo and S. Suga, *J. Phys. Chem. B*, 2005, **109**, 15476.
12 T. Horiuchi, H. Miura and S. Uchid, *Chem. Commun.*, 2003, 3036.
13 (*a*) M. Velusamy, K. R. J. Thomas, J. T. Lin, Y. Hsu and K. Ho, *Org. Lett.*, 2005, **7**, 1899; (*b*) D. P. Hagberg, T. Edvinsson, T. Marinado, G. Boschloo, A. Hagfeldt and L. Sun, *Chem. Commun.*, 2006, 2245.
14 (*a*) D. P. Hagberg, T. Marinado, K. M. Karlsson, K. Nonomura, P. Qin, G. Boschloo, T. Brinck, A. Hagfeldt and L. Sun, *J. Org. Chem.*, 2007, **72**, 9550; (*b*) P. Qin, H. Zhu, T. Edvinsson, G. Boschloo, A. Hagfeldt and L. Sun, *J. Am. Chem. Soc.*, 2008, **130**, 8570; (*c*) H. Qin, S. Wenger, M. Xu, F. Gao, X. Jing, P. Wang, S. M. Zakeeruddin and M. Grätzel, *J. Am. Chem. Soc.*, 2008, **130**, 9202; (*d*) H. Tian, X. Yang, R. Chen, R. Zhang, A. Hagfeldt and L. Sun, *J. Phys. Chem. C*, 2008, **112**, 11023; (*e*) Z. Ning, Q. Zhang, W. Wu, H. Pei, B. Liu and H. Tian, *J. Org. Chem.*, 2008, **73**, 3791; (*f*) H. Choi, C. Baik, S. O. Kang, J. Ko, M.-S. Kang, M. K. Nazeeruddin and M. Grätzel, *Angew. Chem., Int. Ed.*, 2008, **47**, 327; (*g*) P. Bonhôte, J.-E. Moser, R. Humphry-Baker, N. Vlachopoulos, S. M. Zakeeruddin, L. Walder and M. Grätzel, *J. Am. Chem. Soc.*, 1999, **121**, 1324.
15 S. Ito, S. M. Zakeeruddin, R. Humphry-Baker, P. Liska, R. Charvet, P. Comte, M. K. Nazeeruddin, P. Pe′chy, M. Takata, H. Miura, S. Uchida and M. Grätzel, *Adv. Mater.*, 2006, **18**, 1202.
16 (*a*) D. Demeter, P. Blanchard, M. Allain, I. Grosu and J. Roncali, *J. Org. Chem.*, 2007, **72**, 5285; (*b*) N. Fukuri, N. Masaki, T. Kitamura, Y. Wada and S. Yanagida, *J. Phys. Chem. B*, 2006, **110**, 25251; (*c*) M. Melucci, P. Frere, M. Allain, E. Levillain, G. Barbarella and J. Roncali, *Tetrahedron*, 2007, **63**, 9774; (*d*) S. G. Im and K. K. Gleason, *Macromolecules*, 2007, **40**, 6552; (*e*) G. Lu, C. Li, J. Shen, Z. Chen and G. Shi, *J. Phys. Chem. C*, 2007, **111**, 5926.
17 H. Choi, J. K. Lee, K. H. Song, K. Song, S. O. Kang and J. Ko, *Tetrahedron*, 2007, **63**, 1553.
18 G. Li, K.-J. Jiang, Y.-F. Li, S.-L. Li and L.-M. Yang, *J. Phys. Chem. C*, 2008, **112**, 11591.
19 S. Roquet, A. Cravino, P. Leriche, O. Alévêque, P. Frère and J. Roncali, *J. Am. Chem. Soc.*, 2006, **128**, 3459.
20 N. Koumura, Z.-S. Wang, S. Mori, M. Miyashita, E. Suzuki and K. Hara, *J. Am. Chem. Soc.*, 2006, **128**, 14256.
21 (*a*) S. Kim, J. K. Lee, S. O. Kang, J. Ko, J.-H. Yum, S. Fantacci, F. De Angelis, D. Di Censo, Md. K. Nazeeruddin and M. Grätzel, *J. Am. Chem. Soc.*, 2006, **128**, 16701; (*b*) M. Liang, W. Xu, F. Cai, P. Chen, B. Peng, J. Chen and Z. Li, *J. Phys. Chem. C*, 2007, **111**, 4465; (*c*) X.-H. Zhang, C. Li, W.-B. Wang, X.-X. Cheng, X.-S. Wang and B.-W. Zhang, *J. Mater. Chem.*, 2007, **7**, 642; (*d*) D. P. Hagberg, J.-H. Yum, H. Lee, F. De Angelis, T. Marinado, K. M. Karlsson, R. Humphry-Baker, L. Sun, A. Hagfeldt, M. Grätzel and M. K. Nazeeruddin, *J. Am. Chem. Soc.*, 2008, **130**, 6259.
22 (*a*) K. R. Justin Thomas, Y.-C. Hsu, J. T. Lin, K.-M. Lee, K.-C. Ho, C.-H. Lai, Y.-M. Cheng and P.-T. Chou, *Chem. Mater.*, 2008, **20**, 1830; (*b*) G. Zhou, N. Pschirer, J. C. Schöneboom, F. Eickemeyer, M. Baumgarten and K. Müllen, *Chem. Mater.*, 2008, **20**, 1808; (*c*) D. Liu, R. W. Fessenden, G. L. Hug and P. V. Kamat, *J. Phys. Chem. B*, 1997, **101**, 2583.
23 A. Hagfeldt and M. Grätzel, *Acc. Chem. Res.*, 2000, **33**, 269.
24 K. Hara, K. Miyamoto, Y. Abe and M. Yanagida, *J. Phys. Chem. B*, 2005, **109**, 23776.
25 J. M. Raimundo, P. Blanchard, N. Gallego-Planas, N. Mercier, I. Ledoux-Rak, R. Hierle and J. Roncali, *J. Org. Chem.*, 2002, **67**, 205.
26 S. Ito, P. Liska, P. Comte, R. Charvet, P. Péchy, U. Bach, L. Schmidt-Mende, S. M. Zakeeruddin, M. K. Nazeeruddin and M. Grätzel, *Chem. Commun.*, 2005, 4351.
27 T. Horiuchi, H. Miura, K. Sumioka and S. Uchida, *J. Am. Chem. Soc.*, 2004, **126**, 12218.
28 M. J. Frisch, G. W. Trucks, H. B. Schlegel, G. E. Scuseria, M. A. Robb, J. R. Cheeseman, J. A. Montgomery, Jr., T. Vreven, K. N. Kudin, J. C. Burant, J. M. Millam, S. S. Iyengar, J. Tomasi, V. Barone, B. Mennucci, M. Cossi, G. Scalmani, N. Rega, G. A. Petersson, H. Nakatsuji, M. Hada, M. Ehara, K. Toyota, R. Fukuda, J. Hasegawa, M. Ishida, T. Nakajima, Y. Honda, O. Kitao, H. Nakai, M. Klene, X. Li, J. E. Knox, H. P. Hratchian, J. B. Cross, V. Bakken, C. Adamo, J. Jaramillo, R. Gomperts, R. E. Stratmann, O. Yazyev, A. J. Austin, R. Cammi, C. Pomelli, J. Ochterski, P. Y. Ayala, K. Morokuma, G. A. Voth, P. Salvador, J. J. Dannenberg, V. G. Zakrzewski, S. Dapprich, A. D. Daniels, M. C. Strain, O. Farkas, D. K. Malick, A. D. Rabuck, K. Raghavachari, J. B. Foresman, J. V. Ortiz, Q. Cui, A. G. Baboul, S. Clifford, J. Cioslowski, B. B. Stefanov, G. Liu, A. Liashenko, P. Piskorz, I. Komaromi, R. L. Martin, D. J. Fox, T. Keith, M. A. Al-Laham, C. Y. Peng, A. Nanayakkara, M. Challacombe, P. M. W. Gill, B. G. Johnson, W. Chen, M. W. Wong, C. Gonzalez and J. A. Pople, *GAUSSIAN 03 (Revision B.03)*, Gaussian, Inc., Wallingford, CT, 2004.

